Proceedings of International Conference on Heat Exchanger Fouling and Cleaning - 2013 (Peer-reviewed)
June 09 - 14, 2013, Budapest, Hungary
Editors: M.R. Malayeri, H. Müller-Steinhagen and A.P. Watkinson
Published online
www.heatexchanger-fouling.com

AN INDUSTRIAL CASE STUDY ON RETROFITTING HEAT EXCHANGERS AND REVAMPING PREHEAT TRAINS SUBJECT TO FOULING

E.M. Ishiyama[1,2*], S.J. Pugh[1], J. Kennedy[1], D.I. Wilson[2] , A. Ogden-Quin[3] and G. Birch[3]

[1] IHS Downstream Research, 133 Houndsditch, EC3A 7BX London, United Kingdom
[2] Department of Chemical Engineering and Biotechnology, University of Cambridge, CB2 3RA Cambridge, United Kingdom
[3] Petroineos, Grangemouth, United Kingdom
*E-mail: Edward.ishiyama@ihs.com

ABSTRACT

Crude refinery preheat trains (PHTs) are a major part of a refining process as these units reduce the amount of thermal energy required to heat the crude oil to its distillation temperature. Fouling is a longstanding problem in the operation of PHTs; the ability of a refinery to process different crude blends or to increase its production capacity depends on the thermal and hydraulic performance of the PHT under fouling conditions. A case study based on a UK refinery preheat train is presented. The fouling behaviour is extracted from the plant's monitoring database, which enabled fouling behaviour to be identified based on operating flows and temperatures. Techno-economic analyses for heat recovery and fouling mitigation, including retrofit of heat exchangers, use of tube inserts, and network revamp, were conducted. The commercial software tool, SmartPM, was successfully utilized to study heat recovery paths, cleaning schedules and furnace firing capacity on this case study.

INTRODUCTION

Crude refinery preheat trains (PHTs) are networks of heat exchangers that transfer heat from process streams to the crude in order to raise its temperature before it enters an atmospheric distillation column for fractional separation. Up to 70% of the heat required is provided by the PHT: the remaining heat is provided *via* a fired heater. Fouling in PHTs is a major economic and environmental problem as it reduces thermal efficiency and throughput capacity of the system. Identifying effective methodologies to manage PHT fouling remains a key research area (Crittenden *et al*., 1992; ESDU, 2000; Panchal and Huangfu, 2000; Ishiyama *et al*., 2013).

A typical PHT includes units such as a desalter and pre-flash tower which are required to operate within a constrained set of operating parameters. The PHT is followed by a fired heater, which itself has a maximum furnace duty limit.

Crude oil fouling is a complex phenomenon. Fouling is caused by different mechanisms at different locations on the PHT, as a consequence of different chemical and physical mechanisms (Lemke, 1999). Chemical reaction fouling is known to be the dominant mechanism downstream of the desalter (Yeap *et al*., 2004). Chemical reaction fouling is the formation of deposits on heat transfer surfaces where the fouling precursors are generated by chemical reaction. Two types of reactions are common: formation of gums (when the sulphur content of the crude is high) and decomposition of maltenes to produce insoluble asphaltenes. Asphaltenes are complex polynuclear aromatic compounds and often the cause for chemical reaction fouling in this part of the preheat train (Lambourn & Durrieu, 1983). Other reactions such as those catalysed by FeS and other corrosion products could also be present.

Water carry over from the desalter can result in rapid fouling of exchangers operating at the temperature at which the water evaporates. These exchangers are easily identified. Careful analysis of monitoring data provides useful diagnostics.

Several quantitative models for calculating (or estimating) crude oil fouling rates have appeared, following the introduction of the 'fouling threshold' concept by (Ebert & Panchal, 1997). This semi-empirical approach, originally introduced to evaluate the rate of crude oil tube-side fouling at a local condition (point condition), describes the fouling rate as the combination of a deposition term and a fouling suppression term. The rate exhibits two primary dependencies: it (i) increases with increasing surface (and film) temperature and (ii) decreases with increasing flow velocity. The concept has become an accepted basis for the development of many heat exchanger design and control strategies as reviewed by (Wilson *et al*., 2005).

Complete mitigation of fouling in refinery PHTs is rarely achieved and periodic cleaning of fouled exchangers is a widely practised approach. The scheduling problem of when and which units to clean have been widely researched within the numerical optimization community (Georgiadis *et al*. 2000; Smaïli *et al*., 2001; Markowski and Urbaniec, 2005; Ishiyama *et al*. 2009; Ishiyama *et al*. 2010).

In this manuscript, the hydraulic aspect of the crude oil fouling is revisited. The crude is pumped *via* centrifugal pumps. These pumps are usually operated under constant rotational speed and are designed to maintain a target throughput even as the network pressure drop increased with fouling. Control of the throughput is achieved through partial opening and closing of the control valves and bypass streams. PHTs can experience hydraulic limitations in two ways: (1) Fouling causes an increase in resistance to flow. If the flow resistance increases to the extent that the centrifugal pump is unable to deliver the required throughput, reduction in throughput will occur with the build-up of foulant (Ishiyama et al., 2009). (2) Fouling reduces the thermal efficiency of the preheat train. This results in the reduction in the coil inlet temperature and increase in the required furnace duty (Lavaja & Bagajewicz, 2005). Once the furnace is unable to deliver the required heat duty, a reduction in throughput will occur to deliver the crude at its target column inlet temperature.

Lavaja & Bagajewicz (2005) discussed a methodology to formulate a cleaning scheduling algorithm, where the reduction in throughput was imposed due to a furnace firing limit. The formulation was based on a non-convex mixed integer nonlinear programming (MINLP) methodology; the study neither employed dynamic fouling models nor a rigorous furnace model.

The aim of this paper is to model dynamic fouling behaviour in an operating PHT and to evaluate furnace firing capacity under different operational strategies. The study enables the identification of exchangers which would result in a greater benefit through retrofit actions, and also to explore possible changes in the network structure.

Commercial computer programs from IHS, SmartPM and EXPRESSplus, were used for this case study. The SmartPM software is built upon the combination of advanced heat exchanger network simulation and cleaning scheduling methodology and industrially accepted shell-and-tube heat exchanger design and rating technology. The network simulation code was developed at the University of Cambridge as part of the EPSRC funded CRude Oil Fouling (CROF) research program. The heat exchanger design technology was developed for the computer program EXPRESSplus and re-implemented in SmartPM. The techniques described in this manuscript are incorporated into SmartPM. SmartPM will hereafter be referred to as 'the simulator'.

MODEL DESCRIPTION

Overall heat transfer coefficient: The thermal performance of individual heat exchangers is modelled using the overall heat transfer coefficient, U, as the sum of thermal resistances in series:

$$\frac{1}{UA_o} = \frac{1}{h_o A_o} + \frac{1}{h_i A_i} + \frac{R_f}{A_{i,cl}} + \frac{R_w}{A_o} \tag{1}$$

Here A_o is the external heat transfer area, A_i is the internal heat transfer area, R_w is the wall resistance, h_i is the internal film transfer coefficient and h_o is the external film transfer coefficient. Subscript 'cl' denotes clean conditions. In this case the heat transfer area related to R_f is taken as A_i (assuming the deposit is forming on the tube-side). If deposition occurs on the shell-side, equation (1) is used taking A_o as the heat transfer area related to R_f.

Fouling rate: The chemical reaction fouling model for tube- or shell-side deposition presented by Polley (2010) was used to quantify the rate of fouling in this study:

$$\left(\dot{R_f}\right)_{crude} = \frac{a}{h_c} exp\left(\frac{-E_a}{RT_f}\right) p \tag{2}$$

Here, $\left(\dot{R_f}\right)_{crude}$ is the rate of crude stream fouling, a is a dimensional constant, h_c, is the film transfer coefficient of the cold (crude) stream (this can be either on the tube- or shell-side), R is the gas constant, T_f is the film temperature and p is an attachment probability based on surface shear stress. For a particular crude slate, 'a' is a constant. E_a is taken as the activation energy for maltene decomposition, 44,300 J mol^{-1} (Wiehe, 2008). The attachment probability term, p, is a function of wall shear stress, τ_w and given by Polley (2010) as:

$$p = 1 - \left(\frac{\tau_w - 2}{98}\right)^{0.5} \qquad \text{When } \tau_w \geq 2 \text{ Pa}$$

$$p = 1 \qquad \text{When } \tau_w < 2 \text{ Pa} \tag{3}$$

The fouling resistance at a given instance t_n, denoted by $R_{f,n}$ could be simulated through use of equation (2) as

$$R_{f,n} = R_{f,n-1} + \left[\left(\dot{R_f}\right)_{crude} + \left(\dot{R_f}\right)_{process}\right] \Delta t \tag{4}$$

Here, $R_{f,t-1}$ is the fouling resistance at time instance 't_{n-1}'. The term, $\left(\dot{R_f}\right)_{process}$, presents the fouling rate of the process stream where applicable.

Furnace duty: The furnace heat duty, Q_f, is presented by

$$Q_f = m[H(T_2, P_2) - H(T_1, P_1)] \tag{5}$$

Here H is the specific enthalpy of the crude at a given temperature (T) and pressure (P). m is the operating crude mass flow rate. Subscripts 1 and 2 denote conditions at the inlet and the outlet of the furnace, respectively.

The maximum throughput, m_{max}, for a maximum furnace capacity, $Q_{f,max}$, is given by

$$m_{max} = \frac{Q_{f,max}}{[H(T_2, P_2) - H(T_1, P_1)]} \tag{6}$$

If the plant is focused to operate at a target throughput, m_{target}, (instead of the maximum as in equation (6)), the following condition is included in the simulation.

$$m = m_{target}, \text{ when } m_{max} \geq m_{target}$$
$$m = m_{max}, \text{ when } m_{max} < m_{target} \tag{7}$$

The variation in the hot stream flow rate is assumed to be proportional to the variation in the crude stream flow rate. Fouling within the fired heater was not considered in this work; this was discussed by Fuentes *et al*. (2011).

Scheduling: The cleaning scheduling formulation is based on the heuristic algorithm formulated by Ishiyama *et al*. (2009). The objective function is to minimize the total economic impact during the operating period:

Total economic cost = Cost of energy + Cost of lost throughput margin + Cost of cleaning (8)

Case study network

The PHT studied is part of the Petroineos refinery at Grangemouth, UK (the refinery is relatively old as its construction dates back to 1950's). The medium and hot sections of the PHT are presented in Figure 1. The crude enters the desalter at around 110 °C and its temperature is raised to ~ 155 °C via exchangers E1 – E2. The crude passes through a flash tower and is then heated to ~ 205 °C, before entering the furnace. The current capacity of the PHT is 52,000 bbl day^{-1}. The coil inlet temperature over a 10 month period is reported in Figure 2(a). During this period a turn-around took place after 7 months where all the units in Figure 1 were cleaned. Before this, the coil inlet temperature had dropped to 170 °C. The throughput over this period (Figure 2(b)) exhibits continuous fluctuation, with a gradual decreasing trend till the plant shutdown.

Design conditions of the exchangers labelled 'E' in Figure 1 are summarized in Table 1. Exchangers E1ab, E1cd, E2abd, E3ab consist of 2, 2, 3 and 2 shells in series, respectively. If these units are to be isolated (*e.g.* during a cleaning action), all shells in series have to be isolated due to the location of the isolation valves. The locations where the temperatures, flows and pressures are monitored are marked in the PHT diagram in Figure 1. Not all stream temperatures and flows are monitored: hence it is necessary to generate the missing information before evaluating the fouling behaviour of each shell. The data reconciliation methodology reported by Ishiyama *et al.*, (2013) and implemented in the simulator was employed to generate automatically the missing stream parameters and the fouling resistance profiles for each shells. The results are summarized in Figure 3.

Table 1: Exchanger design details

	E1a-d	E2a-c	E3ab	E4
Crude stream flow rate, kg s^{-1}	34	31	35	17.5
Hot stream flow rate, kg s^{-1}	12.5	30	20	19
Area per shell, m^{2}	210	190	150	63
Number of tube-side passes	8	2	2	2
U, W m^{-2} K^{-1}	160	70	98	380
h_i, W m^{-2} K^{-1}	670	1060	1120	1670
h_o, W m^{-2} K^{-1}	1330	1423	870	2540
Tube-side velocity, m s^{-1}	0.6	0.7	0.8	1.3

The fouling resistance profiles for shells E1a-d in Figure 3 show a disturbance between the 2nd and 3rd months which corresponds to the disturbance in the volumetric flow of the cold stream to E1a-d evident in (Figure 4). The thermal resistance profiles for each shells are different with higher thermal resistance in the hotter unit (E1a < E1b < E1c < E1d). Following the cleaning event (month 7), the exchangers exhibit a minimum resistance of 0.005 W m^{-2}K^{-1}. The fouling profiles are quasi-linear. When the desalter inlet temperature is not controlled, units downstream can be subject to inorganic salt crystallization fouling (as reported by Ishiyama *et al.* 2010). The desalter temperature here was controlled at around 110 °C throughout the operation, and little carryover of salts from the desalter was expected.

The fouling resistance profiles obtained for exchangers E2abc, E3ab and E4 are plotted in Figure 3. The distribution of the fouling resistances between shells exhibit similar behaviour to E1a-d, where the hotter unit exhibits a higher fouling resistance at a given time. Exchangers E1, 3 and 4 were cleaned on the 7th month during a plant shut-down. The exchangers were cleaned using hydro-blasting. The cleaning action did not achieve perfect cleaning and all exchangers exhibit a residual fouling resistance. The residual fouling resistances extracted for each shell in Figure 3 are reported in Table 2. The observed residual resistances are relatively high, even after a cleaning action. The degree of cleaning could be interpreted via the fouling Biot number, Bi_f, given by,

$$Bi_f = U_{cl} R_f \tag{9}$$

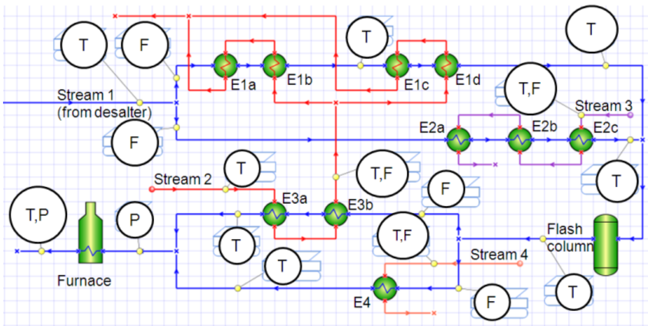

Figure 1: Hot end of the PHT. Label 'E' denotes a heat exchanger. T, F and P present locations where the temperature, flow and gauge pressure are measured.

Table 2 shows exchangers exhibiting Bi_f values greater than 1, indicating even after cleaning the unit performance is less than half of its clean overall heat transfer coefficient. A higher degree of cleaning could be achieved through alternative cleaning methods (*e.g.* use of hydro drilling). It is important to note that the absolute value of R_f is subject to the uncertainties in the stream physical properties, collected data and exchanger geometries.

Table 2: Summary of heat exchanger residual fouling resistances following cleaning

Heat Exchanger	R_f, m^2 K KW^{-1}	Bi_f
E3a	0.25	0.17
E3b	0.6	0.46
E4	0.25	0.3
E2a	3.0	1.9
E2b	4.0	2.7
E2c	5.0	3.5
E1a	5.0	1.4
E1b	5.0	2.6
E1c	4.0	2.0
E1d	3.0	1.7

The slopes of the fouling resistance profiles, *i.e*. the fouling rates, were found to be a strong function of operating temperature and flow rate. Regions of stable operation were identified for each exchanger within the simulator, generating a matrix of operating periods. The corresponding fouling rates and operating data are used to evaluate parameters for fouling models such as equation (2). This allows the modelling of fouling performance in periods where particular crude blends are processed, hence allowing a database of crude slate specific fouling model parameters to be constructed for use in simulation and cleaning calculations. The fouling parameter, a, in equation (2) is evaluated by regression analysis, fitting the value to minimize the sum of differences between the observed and predicted fouling rates using equation (2), for each heat exchanger.

The reliability of the fitted fouling model parameter was tested through simulating the historical performance using the observed inlet conditions and the initial fouling resistances as inputs for the network. The simulation results are plotted as dashed lines in Figure 3 using equations (2) and (4) with a = 450 h^{-1}. With the exception of E3a (Figure 3(j)), the simulated fouling profiles matches the reconciled data well. A possible reason for the discrepancy for E3a, where R_{f} is under predicted by equation (2) is that process stream fouling is occurring, which could be accounted for separately:

$$\left(\dot{R_f}\right)_{total} = \left(\dot{R_f}\right)_c + \left(\dot{R_f}\right)_{process} \tag{10}$$

Here, $\left(\dot{R_f}\right)_{total}$, gives the total fouling rate of the exchanger, $\left(\dot{R_f}\right)_{crude}$ is given by equation (2) and $\left(\dot{R_f}\right)_{process}$ is the fouling rate on the process side. The vacuum residue stream is known to the refinery to cause severe fouling. Fouling of exchanger E3 by this stream has not been visually confirmed, but we have acknowledged this possibility based on past refinery experience.

During the data reconciliation period, the PHT was operated to achieve a target throughput. Due to the furnace reaching its maximum capacity, a gradual reduction in throughput has occurred. The operating condition of the furnace is summarized in Table 3.

Taking the PHT operating parameters at the beginning of the data reconciliation period as the starting point, the CIT and throughput profiles were simulated (solid lines in Figure 2). A target throughput of 85 kg s^{-1} was assumed, which would decrease if the furnace is unable to provide the required duty; the throughput was obtained using the conditions given by equation (7) together with equations (5) and (6). The cleaning actions were not taken into account. There are three distinct sections in the simulated throughput graph Figure 2(b). Section AB is a region of constant throughput, where the furnace is able to accommodate the reduction in CIT at the target throughput, as the furnace has not reached its duty limit. Section BC presents a region where there has been a reduction in throughput as a consequence of the furnace reaching its maximum duty with fouling.

Figure 3 shows that the fouling model, together with the crude thermodynamic data, network simulation model and furnace model, was able to predict the historical plant behaviour. Simulation studies of future performance are now executed to evaluate the best methodology to manage fouling the PHT. In the case studies the objective of the PHT is to operate at maximum throughput (in contrast to a target throughput); hence only equations (5) and (6) are used to evaluate the throughput rather than equation (7).

Case study 1: Simulation and scheduling of the original network with a specified maximum furnace heat duty.

This study evaluated the scenario where the PHT is operated without any cleaning or modifications to the network. This was done by taking the reconciled data set one month after the turn-around obtained from reconciled result as the starting point (Table 4). During this period the crude processed had an average API gravity of around 33 °API. The thermo-physical properties of the streams are detailed in Table 6. The furnace operating condition is given in Table 3. Operation was predicted for a period of 31 months. At the start the furnace is operating at its maximum duty. Hence with the decrease in PHT thermal efficiency (solid line in Figure 5(a)), throughput reduction as fouling occurs (solid line in Figure 5(b)).

Table 3: Furnace performance

Parameter	Value
Maximum capacity	50 MW
Furnace outlet temperature	360 °C
Furnace inlet pressure	9 bara
Furnace outlet pressure	2 bara

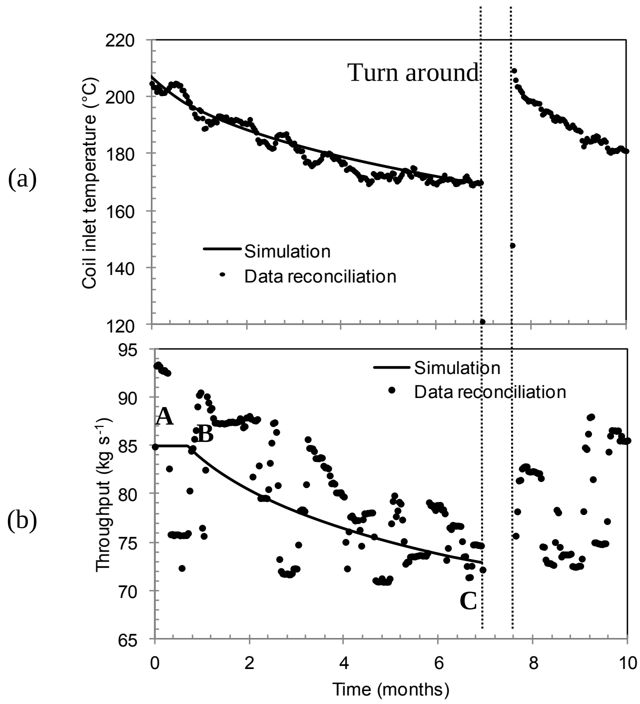

Figure 2: Variation in (a) coil inlet temperature and (b) throughput with time. Symbols represent reconciled data. Solid line shows simulation trend.

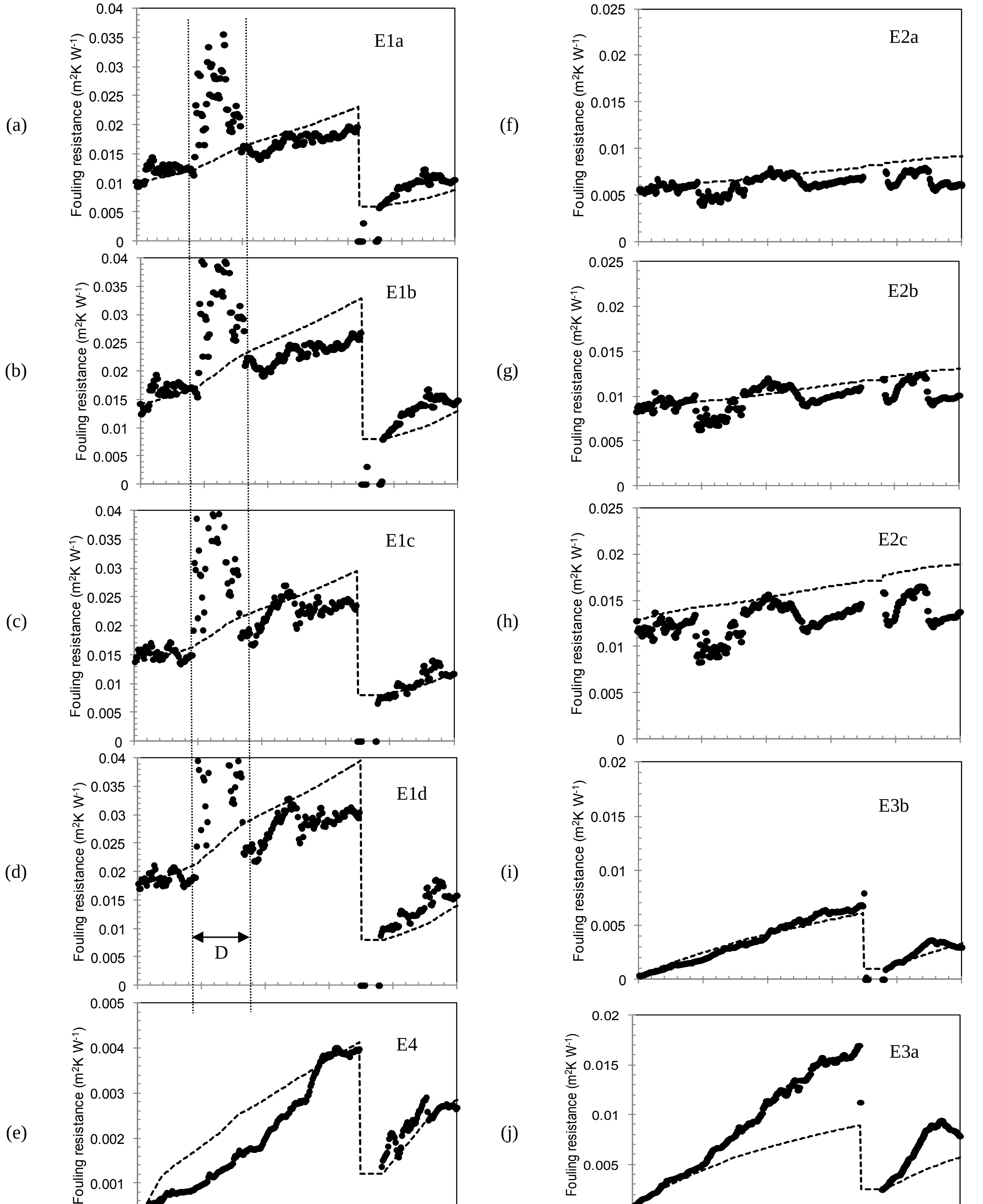

Figure 3: Fouling resistance profile for exchangers E1ab, 2abc, 3ab and 4. Symbols represent reconciled data. Dashed line shows simulation using the fouling model [equation (2)]. 'D' marks period of disturbances to crude inlet temperature measurements.

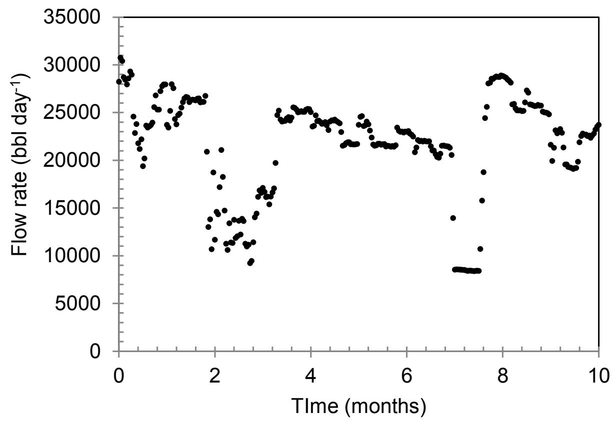

Figure 4: Measured volumetric flow of the crude stream across exchangers E1a-d.

The reduction in throughput, from 85 kg s^{-1} to below 60 kg s^{-1} during the 31 month simulation period, represents significant loss in margin. Now consider cleaning as a mitigation strategy. Each heat exchanger is considered to take 7 days to clean. The optimum cleaning schedule generated for this network indicates that exchanger E3ab requires frequent cleaning. These units have the largest duty in the network and are also the units with fastest fouling (Figure 7). In this paper the retrofit focuses on identifying opportunities on reducing the rate of fouling and to enhance energy recovery (which will consequently increase the throughput under limited furnace duty). The following opportunities were identified:

1. Use of tube inserts for E3ab: E3ab is a major component in the PHT and also subject to severe fouling. Tube inserts were identified as an option to increase the tube-side wall shear stress, which would reduce the rate of fouling. Twisted tapes were selected on the basis of the allowable pressure drop and the ease of installation. Furthermore, twisted tapes could be fabricated onsite.

2. Divert all crude flow rates to E3ab after the pre-flash: The exchanger, E4, has the smallest duty in the network. If there is sufficient cooling water duty available to cool Stream 4, the diversion of crude to E3ab will further increase the wall shear stress to reduce fouling in a long term. Exchanger E4 could be utilized elsewhere in the system (e.g. upstream of the pre-desalter section to maintain desalter inlet temperature).

The suitability and benefits of the above opportunities are explored in the following case studies.

Table 4: Inlet conditions to the preheat train in Figure 1

Stream	Temperature, °C	Flow rate, kg s^{-1}
Stream 1	113	93
Stream 2	315	31
Stream 3	254	62
Stream 4	269	17

Case study 2: Installation of tube inserts to E3ab

Ideally, retrofit options minimize disruption to plant operations. Changes include a different bundle geometry or the use of tube-inserts, which can be done offsite. Here we consider the use of tube-insert for E3ab. Twisted tapes are in common use due to their easy fabrication. An insert with 360° twist over a 100 mm length is considered here. Helical coil wire is also considered in parallel to the twisted tapes. hiTRAN is another common tube-insert which is able to maintain particulates in suspension; it is commonly employed in non-fouling situations to improve heat transfer.

For a crude stream flow rate of 35 kg s^{-1}, the film transfer coefficient and pressure drop comparisons with and without tube-inserts are given in Table 5.

Use of tube-inserts increases the tube-side pressure drop. E3 has 2 tube-side passes but the allowable pressure drop on the tube-side (70 kPa) was greater than the pressure drop with tube-inserts (54 kPa for twisted tapes). The actual variation of pressure drop in E3a is plotted in Figure 6; the reduction in pressure drop is caused by the furnace reaching its maximum firing capacity and throughput being throttled back accordingly. In cases where the tube-inserts raised the pressure drop above the allowable limit, the tube-sheets would have to be modified in order to operate at a reduced number of tube-side passes. This would have been the case if tube-inserts had been used on E1ab and E1cd to enhance heat recovery from Stream 2. The use of tube-inserts on E1ab and E1cd was not recommended in the study as stream 2 leaves E1ab and E1cd enters the cold section of the PHT immediately before the desalter (not shown in Figure 1. Further enhanced heat recovery from stream 2 on the hot end reduced heat recovery in the cold end, and would have an adverse effect on the desalter inlet temperature.

Case study 3: Installation of tube inserts to both E3ab and E2abc and diverge all crude stream across E3ab after the pre-flash

The cold stream flow between E3ab and E4 is split, on average in the ratio 3:1. The ratio of exchanger areas E3ab:E4 is 5:1. The contribution of the E4 heat duty to the network is very small (Figure 7). If the pressure drop allows, the rate of fouling in E3ab could be further reduced through increasing shear; this can be achieved through removing E4 and completely diverting its flow to E3ab. For case studies 1 and 3, the pressure drop contribution of the heat exchangers to the network is plotted in Figure 8. This shows that the increase in network pressure drop is in the range 30 – 40 kPa for case study 3. The allowable pressure drop across E3ab alone (70 kPa) is able to accommodate this increase in pressure drop.

Table 5: Comparison of h_i and pressure drop for E3ab (allowable tube-side pressure drop 70 kPa)

	Plain tube	Twisted tape
h_i, (W m^{-2} K^{-1})	1120	2170
ΔP (kPa)	9.6	54.1

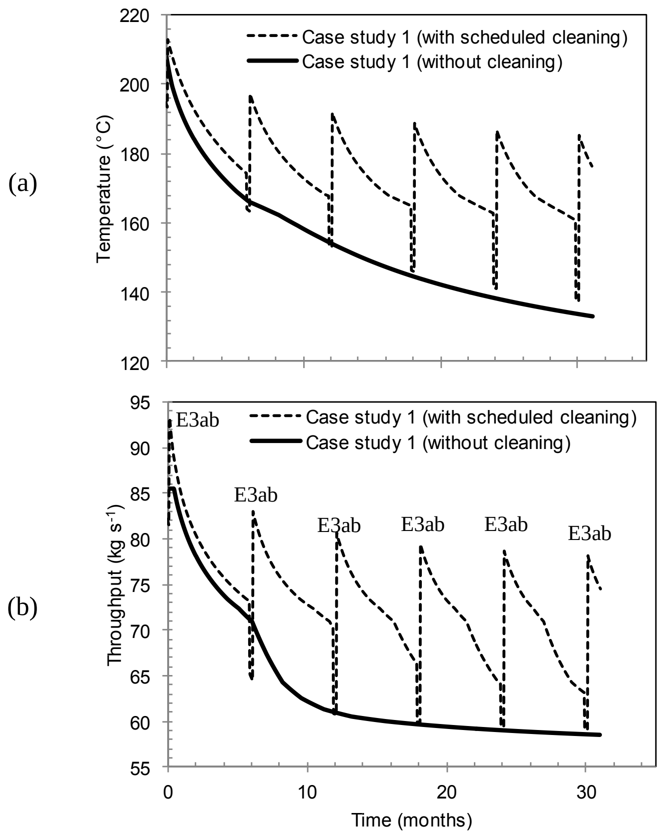

Figure 5: Case study 1: Evolution of (a) temperature and (b) throughput. Simulation of future performance without modification to the network. The cleaning actions indicate where E3ab is cleaned.

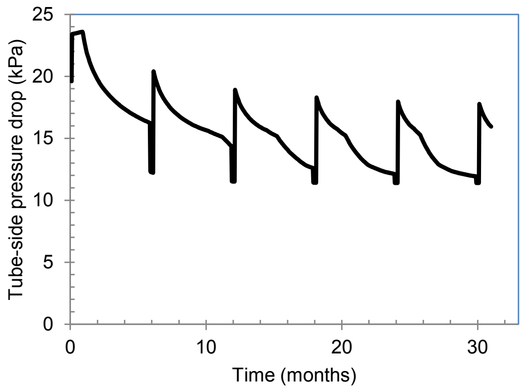

Figure 6: Case study 1: Variation of tube-side pressure drop for shell E3a.

DISCUSSION

Figure 9 compares the CIT and throughput profiles for the case studies, if no cleaning actions were performed during the simulation period. The immediate benefit in increased CIT is highest for case study 2. This is also reflected in a higher starting throughput at the maximum furnace capacity. The CIT is initially lower for case study 3, compared to case study 2, as case study 3 starts the operation without exchanger E4. The differences in gradient indicate that with tube-inserts and with higher flow rate, the impact of fouling to the PHT performance is reduced. The benefit of case studies 2 and 3 are immediately evident through the initial increase in CIT and subsequent reduced rate of decrease in both CIT and throughput. Case study 3 proves to be superior over a longer operating period as it offers the lowest overall fouling rate in E3ab and the total throughput is largest.

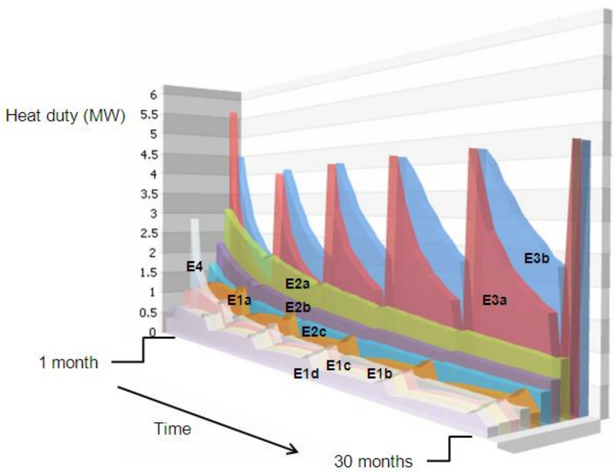

Figure 7: Variation of exchanger heat duty over time.

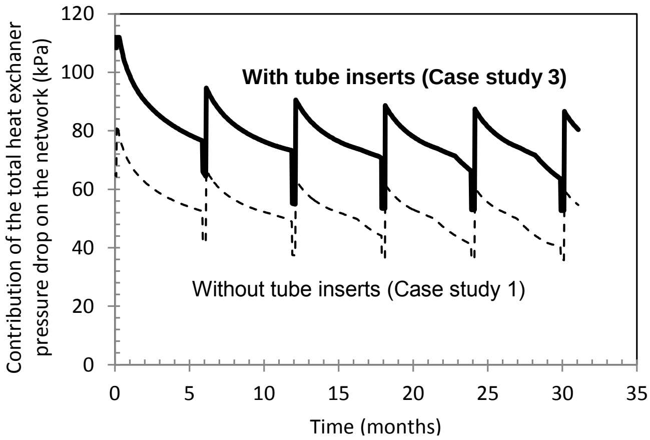

Figure 8: Contribution of the total heat exchanger pressure drop on the network. Dashed and solid bold lines show case studies 1 and 3, respectively.

The economic benefits of the case studies are compared over the 31 month period by taking case study 1 (without cleaning) as the base case. As the furnace is operating at its maximum duty, any difference in the economic performance is directly related to the throughput processed.

Difference in benefit =

$$C_{lo} \int_{0}^{t_f} (m_j - m_{reference})\, dt \; - total\ cleaning\ cost \qquad (11)$$

Here, m is the PHT throughput, C_{lo} is the throughput margin, subscript 'j' denotes case studies 1 to 3, and subscript 'reference' denote case study 1 under no cleaning condition. t_f denote the time duration where the scheduling study was performed.

The economic benefit calculated using equation (11), with a throughput margin, C_{lo}, of 2 US$ per bbl are summarized in Table 7. Over a longer term, case study 4, combined with cleaning gives superior benefit compared to case study 1 of ~ 4 MM US$. (*i.e*. 15.24 – 11.30 MM US$). Both case studies 2 and 3 show simple retrofit options, with considerable immediate financial benefits. It is observed from Table 7, that the combination of retrofit and optimized cleaning gives a financial benefit at least three times greater than that of retrofit action alone.

CONCLUSIONS

1. Plant monitoring data were reconciled to generate fouling resistance profiles for each shell.
2. A dynamic fouling rate model with parameter a = 450 h^{-1} was identified and give reliable simulation of PHT performance.
3. A furnace model was implemented, which enabled the simulation of the reduction in throughput with fouling under operation of maximum furnace duty.
4. Simple retrofit actions together with optimised scheduling were successfully shown to significantly reduce losses due to fouling. Optimised cleaning gave a benefit in improvement at least three times larger than a benefit base on hardware modifications alone.

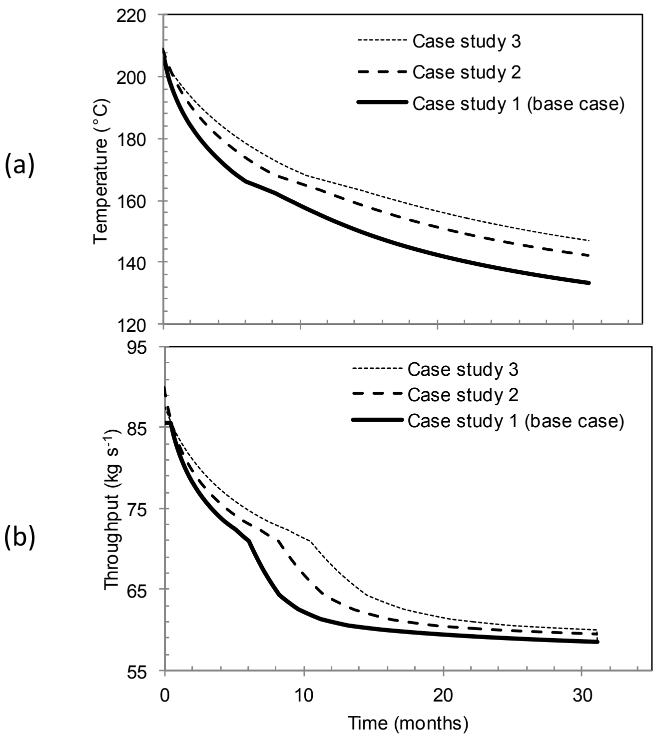

Figure 9: Comparison of case studies 1 to 3, without cleaning actions. Variation in (a) temperature and (b) throughput with time.

Nomenclature

a pre exponential factor, s^{-1}
A heat transfer area, m^2
Bi_f fouling Biot number, -
C_{lo} throughput margin, US$ kg^{-1}
E activation energy, J mol^{-1}
h film transfer coefficient, W m^{-2} K^{-1}
H specific enthalpy of the crude, J kg^{-1}
m mass flow rate, kg s^{-1}
P pressure, bar
p attachment probability, -
Q_f furnace duty, W
R gas constant, J mol^{-1} K^{-1}
R_f fouling resistance, m^{2}K W^{-1}
$\dot{R}_f$ fouling rate, m^{2}K J^{-1}
R_w wall resistance, m^{2}K W^{-1}
t_f time period for simulation, s
T_f film temperature, K
U overall heat transfer coefficient, W m^{-2} K^{-1}

Greek

τ_w wall shear stress, Pa

Subscripts

c crude stream
cl clean condition
i internal
j case study 1, 2, 3 or 4
max maximum
o external
process process stream
total total rate

References

Crittenden, B. D., Kolaczkowski, S. T., & Downey, I. L. (1992). Fouling of crude oil preheat exchangers. *Chem. Eng. Res. Des.*, *70*(A6), 547–557.

Ebert, W. A., & Panchal, C. B. (1997). Analysis of Exxon crude-oil slip stream coking data. In *Fouling Mitigation of Industrial Heat Exchange Equipment* (pp. 451–460), Panchal C.B. (editor), New York: Begell House.

ESDU. (2000). *Exchanger fouling in the pre-heat train of a crude oil distillation unit* (Data Item 00016). IHS ESDU International plc., London.

Fuentes, A. M., Rodriguez, G. M., Polley, G. T., Picon-Nunez, M., & Ishiyama, E. M. (2011). Simplified analysis of influence of preheat train performance and fired heater design on fuel efficiency of fired heaters, 9th International Conference on HEFC, Crete, Greece.

Georgiadis, M. C., Papageorgiou, L. G., & Macchietto, S. (2000). Optimal cleaning policies in heat exchanger networks under rapid fouling. *Ind. Eng. Chem. Res.*, *39*(2), 441–454.

Ishiyama, E. M., Paterson, W. R., & Wilson, D. I. (2009). Platform for techno-economic analysis of fouling mitigation options in refinery preheat trains. *Energy and Fuels*, *23*(3), 1323–1337.

Ishiyama, E. M., Heins, A. V., Paterson, W. R., Spinelli, L., & Wilson, D. I. (2010). Scheduling cleaning in a crude oil preheat train subject to fouling: Incorporating desalter control. *Appl. Thml. Eng.*, *30*(13), 1852–1862.

Ishiyama, E. M., Pugh, S. J., Paterson, B., Polley, G. T., Kennedy, J., & Wilson, D. I. (2013). Management of crude preheat trains subject to fouling. *Heat Transfer Engineering*, *34*(8-9), 692–701.

Lambourn, G. A., & Durrieu, M. (1983). Fouling in crude oil preheat trains, in Heat Exchangers Theory and Practice (p841–852), Taborek J., Hewitt G.F. and Afgan N. (editors), Hemisphere publishing company, NY.

Lavaja, J. H., & Bagajewicz, M. J. (2005). On a new MILP model for the planning of heat-exchanger network cleaning. Part II: Throughput loss considerations. *Ind. Eng. Chem. Res.*, *44*(21), 8046–8056.

Lemke, H. K. (1999). An overview about mechanisms and mitigation of fouling in refinery units. Presented at the AIChE Spring Meeting, Houston.

Markowski, M., & Urbaniec, K. (2005). Optimal cleaning schedule for heat exchangers in a heat exchanger network. *Appl. Thml. Eng.*, *25*(7), 1019–1032.

Panchal, C. B., & Huangfu, E.-P. (2000). Effects of mitigating fouling on the energy efficiency of crude-oil distillation. *Heat Transfer Engineering*, *21*(3), 3–9.

Polley, G. T. (2010). Review of the development of models for the prediction of fouling rates in exchangers heating crude oil (p13–17), 11th International Conference on Petroleum Phase Behavior and Fouling, NJ, USA.

Smaïli, F., Vassiliadis, V. S., & Wilson, D. I. (2001). Mitigation of fouling in refinery heat exchanger networks by optimal management of cleaning. *Energy and Fuels*, *15*(5), 1038–1056.

Wiehe, I. A. (2008). *Process Chemistry of Petroleum Macromolecules*. US: CRC Press. p132.

Wilson, D. I., Polley, G. T., & Pugh, S. J. (2005). Ten years of Ebert, Panchal and the 'threshold fouling' concept. 6th International Conf. on HEFC. Kloster, Irsee, Germany.

Yeap, B. L., Wilson, D. I., Polley, G. T., & Pugh, S. J. (2004). Mitigation of crude oil refinery heat exchanger fouling through retrofits based on thermo-hydraulic fouling models. *Chem. Eng. Res. Des.*, *82*(1), 53–71.

Table 6: Stream thermo-physical properties

	Density, kg m^{-3} = b_1 *(T-273)*+ b_2	Thermal conductivity, W m^{-1} K^{-1} = c_1 *(T-273)* + c_2	Specific heat capacity, J kg^{-1} K^{-1} = d_1 *(T-273)* + d_2	Viscosity, cP = e_1 *exp*(e_2 */T*)
Stream	b_1 (kg m^{-3} K^{-1}), b_2 (kg m^{-3})	c_1(W m^{-1} K^{-2}), c_2 (W m^{-1} K^{-1})	d_1(J kg^{-1} K^{-2}), d_2 (J kg^{-1} K^{-1})	e_1 (Pa s), e_2 (K)
1	-0.890, 871	-0.0004, 0.164	3.462, 1945	6.677E-03, 1952.11
2	-0.819, 878	-0.0002, 0.169	3.467, 1900	3.437E-03, 2193.37
3	-1.091, 956	-0.0015, 0.125	5.45, 1518	3.081E-03, 2256.01
4	-0.683, 837	-0.0002, 0.157	2.889, 2073	3.081E-03, 2256.01

Table 7: Comparison of the economic benefit for the case studies 1 – 3 over a period 31 month.

	Benefit (from equation (11)) MM US$	
	Without cleaning	With cleaning
Case study 1: Base case	0.00 (base case)	11.30
Case study 2: Installation of tube-inserts to E3ab	2.39	12.95
Case study 3: Installation of tube-inserts to E3 and E2abc and flow diversion	4.25	15.24